Super-Wettability | Special Issue 150 Years of BASF

DOI: 10.1002/anie.201409911

Bioinspired Super-Wettability from Fundamental Research to Practical Applications

*Liping Wen, Ye Tian, and Lei Jiang**

Keywords:
bio-inspired materials · interfaces · surface chemistry · wettability

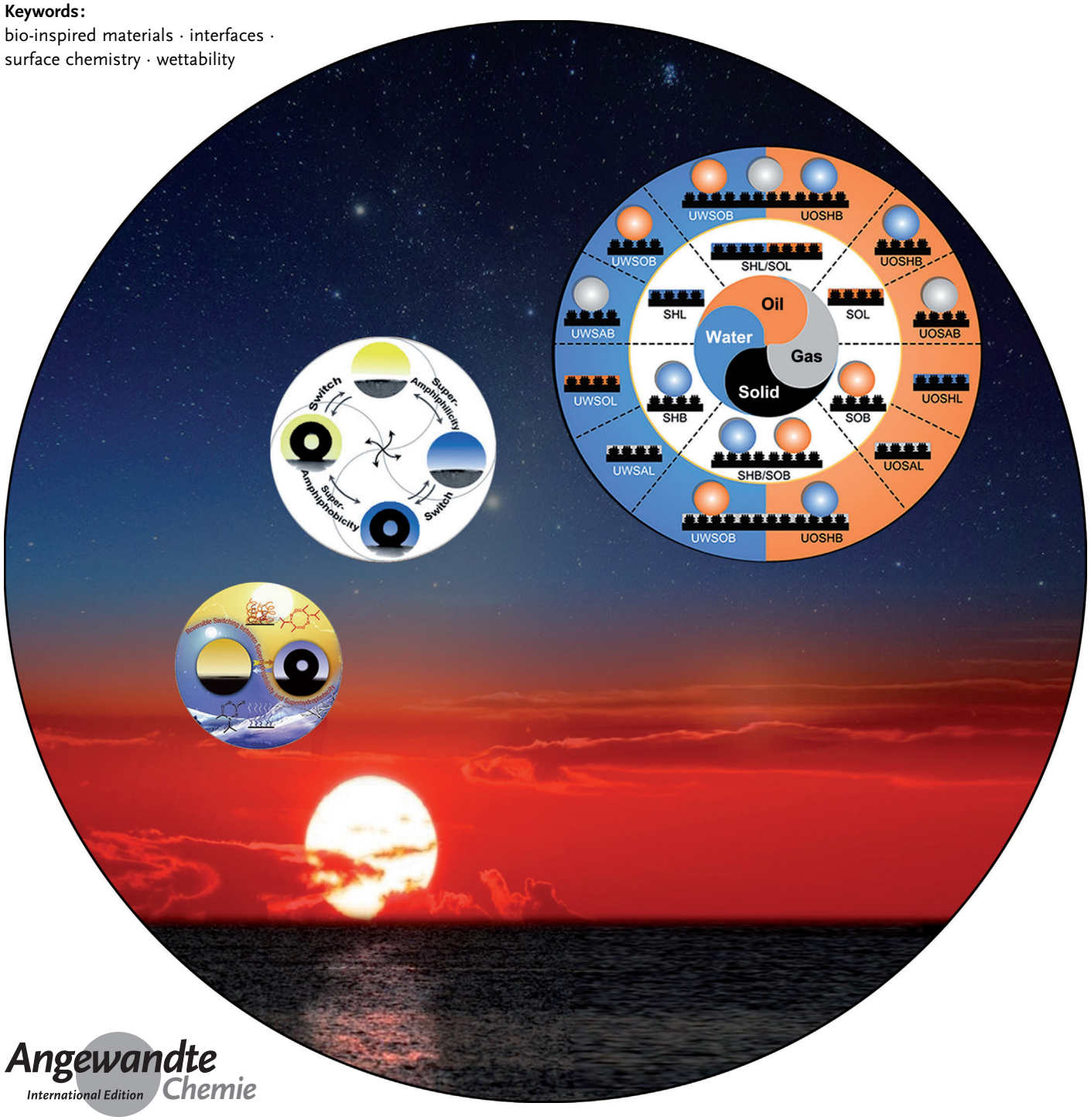

Angewandte International Edition Chemie

Engineered wettability is a traditional, yet key issue in surface science and attracts tremendous interest in solving large-scale practical problems. Recently, different super-wettability systems have been discovered in both nature and experiments. In this Review we present three types of super-wettability, including the three-dimensional, two-dimensional, and one-dimensional material surfaces. By combining different super-wettabilities, novel interfacial functional systems could be generated and integrated into devices for use in tackling current and the future problems including resources, energy, environment, and health.

From the Contents

1. Introduction 3388

2. Theoretical Basis 3388

3. Application of Super-Wettability Surfaces 3389

4. Summary and Outlook 3397

1. Introduction

Wettability is a fundamental property of a solid surface and is currently a hot topic and plays a key role in addressing the problems related to energy, environment, resources, and health. Research on the interface between solid materials and liquids or fluids was initiated in 1805 and resulted in the Young's equation which provided a basis for further study of wettability.[1] Since then, different models and principles have been developed, of which several are now widely accepted and used to direct current practice. In 1907, Ollivier first reported a super-antiwetting surface by coating a substrate with soot, the resulting contact angle was nearly 180°,[2] while the concept of superhydrophobic surfaces received gradual interest until 1997, when the explanation of the origin of the "lotus effect" in nature was provided by Barthlott and Neinhuis.[3] They thought the self-cleaning effect related to the micrometer-scale papillae and the epicuticular wax. Five years later, an more accurate mechanism of the function of such a superhydrophobic surface, which incorporates chemical compositions and the surface geometrical structures was reported based on studying the lotus leaf.[4] Other biological surfaces have been found to display super-wettability, including the rice leaf,[4] desert beetle's back,[5] water strider's leg,[6] spider silks,[7] and fish scales.[8] These surfaces provide inspiration for the design, fabrication, and application of super-wettability surfaces. From a global research report of materials science and technology published in 2011 (Figure 1 A),[9] the total citation of superhydrophobic surfaces was ranked seventh among 438 current activities which in chemistry, physics, engineering, and biological sciences. This evaluation confirms that superhydrophobicity in air is a major topic but also has potential applications related to the material surfaces. Notably, if the superhydrophobic surfaces in air were extended to the water and oil systems, more achievements will be obtained in the future.

Furthermore, by searching in ISI Web of Science for the topic of super-wettability, an accelerating increase in the number of papers published each year is found (Figure 1 B). Besides superhydrophobicity in air, super-wettability also covers: superhydrophilicity, superoleophobicity, and superoleophilicity in air (see middle part in Figure 2); under-oil superhydrophobicity, superhydrophilicity, superaerophobicity and superaerophilicity (see right part in Figure 2); underwater superoleophobicity, superoleophilicity, superaerophobicity and superaerophilicity (see left part in Figure 2).[10] Although many achievements have been made involving superhydrophobic surfaces, from the fundamental research to practical applications,[11–15] further efforts should be made to extend the applications of other super-wettability surface systems (Figure 2).

2. Theoretical Basis

Wettability is influenced by the chemical composition and the topographical structure of surfaces,[16,17] thus super-wettability surfaces can be constructed by changing these two factors. For a static and flat substrate, the wettability is determined by the surface free energy which is given by the Young's equation [Eq. (1)].[1]

$$\gamma_{sv} = \gamma_{sl} + \gamma_{lv}\cos\theta \quad (1)$$

Herein, θ is the contact angle in the Young's mode, and γ_{sv}, γ_{sl}, and γ_{lv} are the different surface tensions (solid/vapor, solid/liquid, and liquid/vapor) involved in the system. In reality, few solid surfaces are truly flat; therefore, the surface roughness factor should also be considered when evaluating the surface wettability. The theoretical models that are commonly used in roughness surfaces are the Wenzel model,[18] the Cassie model,[19] and the transition between the Wenzel and Cassie model.[20] In the Wenzel model (Figure 3 A), the difference in the measured θ^* is a little different from the contact angle measured on flat surfaces [Eq. (2)].

$$\cos\theta^* = R\cos\theta \quad (2)$$

where R is the roughness of the actual surface whose value is always larger than 1, which means the introduction of R will always provide enhanced surface wettability. In this model, surface roughness can promote either wettability ($\theta_{CA} < 65°$; CA = contact angle) or non-wettability ($\theta_{CA} > 65°$), depending on the chemical composition of the material.[21,22] On the

[*] Dr. L. Wen, Dr. Y. Tian, Prof. L. Jiang
Beijing National Laboratory for Molecular Sciences (BNLMS)
Key Laboratory of Organic Solids, Institute of Chemistry
Chinese Academy of Sciences
Beijing 100190 (P.R. China)
E-mail: jianglei@iccas.ac.cn

basis of superhydrophobicity, the Wenzel model can also be extended to other super-wettability systems, such as superoleophobicity in air, underwater superoleophobicity and superaerophobicity, and under-oil superhydrophobicity and superaerophobicity.

However, if the surface is composed of small protrusions that cannot be filled by the liquid and are thus filled with air (i.e., trapping of air underneath the liquid droplet), the wetting phenomenon can be described by the so-called Cassie–Baxter model [Eq. (3)] (Figure 3B; also called Cassie's mode):

$$\cos\theta^* = f_1\cos\theta_1 + f_2\cos\theta_2 \quad (3)$$

Where θ_1 and θ_2 are the apparent contact angles of the liquid droplet upon the surface 1 and surface 2, respectively. f_1 and f_2 are the apparent area ratios of surface 1 and surface 2 ($f_1 + f_2 = 1$). Clearly, the corresponding θ^* is always higher than that of a flat surface made from the same material because the pores are filled with air, which is used by the Cassie model to describe the contact angle in a liquid/gas/solid system. Such a model can also describe the situation in the oil/water/solid system. In this case, the rough surface is composed of solid and water, and the Cassie model can be expressed as follows (Figure 3C):

$$\cos\theta_{o'} = f\cos\theta_o + f - 1 \quad (4)$$

where f is the surface fraction of solid, θ_o is the contact angle of an oil droplet on a flat surface in water, and $\theta_{o'}$ is the contact angle of an oil droplet on a rough surface in water. In the water/oil/solid system, the wettability of a solid surface by an oil droplet can be commonly evaluated through the above modified Young's equation (Equation (1)). Therefore, surface roughness can still be considered by a revised Cassie model. If a spherical liquid droplet in Cassie mode is pressed physically, the solid/liquid contact mode will change from the Cassie to the Wenzel state. This change indicates that in addition to coexisting, a transition between these two super hydrophobic states can also occur (Figure 3D). In the dynamic case, however, this wettability is characterized by the advancing contact angle (θ_{Adv}) and the receding contact angle (θ_{Rec}). Both of them are dependent on the adhesion of the materials (Figure 3E). In general, superhydrophobicity means a high θ_{CA} with a low contact-angle hysteresis which is characterized by $\theta_{Adv}/\theta_{Rec}$ or the sliding angle θ_{SA} (Figure 3F).

3. Application of Super-Wettability Surfaces

3.1. Application of Two-Dimensional Super-Wettability Surfaces

3.1.1. Anti-Wetting

With the increasing demand for smart surfaces, much research is focusing on the development of water-repellent surfaces which can display many properties, such as self-cleaning (Figure 4A),[23,24] anti-fogging (Figure 4B),[25,26] anti-reflection,[27,28] anti-corrosion (Figure 4C),[29,30] and biological applications.[31] The commonly used materials for these applications contain textiles,[32–34] glass,[35–38] metal and their alloys[39–41] whose surfaces can be protected from being wetted, contaminated, or fouled by water and oil pollutants. To date, many materials have been used to fabricate these self-cleaning textiles, these include water-repellent silicone,[23] polydimethylsiloxane,[42] sol–gel materials,[43] and photocatalytic titania nanoparticles.[44]

In addition to introducing low-surface-energy coatings, another way to prepare water-repellent surfaces is by increasing surface roughness which can be realized by plasma etching. Our group previously developed a two-step technique including plasma treatment and chemical modification of fluorocarbons to obtain self-cleaning super-amphiphobic (superhydrophobic and superoleophobic) textiles (Figure 4A).[24] To date, many commercial products consisting of self-cleaning textile fabrics have been developed, however endowing these textiles with good durability for washing, sunlight, and high- or low-temperature exposure would be advantageous and also remains a challenge.

Apart from the self-cleaning property used in textiles, the anti-wetting property could also be used as anti-fogging[23,24] and anti-reflective[27,28] materials which could be used in buildings and optical materials, such as windows for high buildings, electronic devices, eyeglasses, optical mirrors and lenses. The most commonly used technique is to coat titanium dioxide onto the outer surfaces, which can give not only a self-cleaning but also an anti-fogging effect (Figure 4B).[35–38] To prepare optical transparency or antireflective surfaces, the key step is to increase the surface roughness. For example, Nakajima et al. developed a transparent surface with self-cleaning properties by controlling the surface roughness in the range of approximately 30–100 nm.[25] The anti-wetting surface can prevent moisture and dirt accumulation and make the surface slippery and abrasion-resistant, thus it is an effective way to increase the device efficiency. Furthermore,

Liping Wen an associate professor at the Institute of Chemistry, Chinese Academy of Sciences (ICCAS). He received his MS degree in organic chemistry from Liaoning Normal University in 2007, where he studied Ciprofluoxacin derivatives. Then he joined Prof. Lei Jiang's group and received his Ph.D. in physical chemistry from ICCAS in 2010. Then he worked with Prof. Tomokuzu Iyoda as a visiting scholar in Japan for three months. His current scientific interests are the construction and application of biomimetic smart membranes.

Ye Tian is an associate professor at the Institute of Chemistry, Chinese Academy of Sciences (ICCAS). She received her B.S. degree from Northeast Normal University (Changchun, China) in 2006. Then she joined Prof. Lei Jiang's group and received her Ph.D. in physical chemistry from ICCAS in 2011. Her scientific interests are focused on biomimetic smart single nanochannels.

making metal surfaces anti-wetting can also prevent their oxidation and corrosion (Figure 4C).[29] However, for some heavily polluted environments, these self-cleaning materials are inefficient, therefore, multi-functional, antipollution self-cleaning products need to be developed to meet future demands.

3.1.2. Anti-Icing

Creating anti-icing surfaces (Figure 4D) has long been a technological challenge and freezing is well known to cause serious problems in aviation, space flight, radar, and transport. Adherent ice can even result in problems that can lead to the destruction of transport vehicles. For example, the cold vapor in the upper-air layers can easily condense and subsequently freeze on the surfaces of a wing, which results, in the worst case, in a dramatic decrease of the lifting force and may lead to a disaster. Thus a water-repellent and self-cleaning superhydrophobic surface could reduce ice adhesion or delayed freezing, and would have great potential to address the icing challenge. Quéré and co-workers reported that freezing of water droplets could be remarkably delayed on cold microtextured superhydrophobic surfaces.[51] Conversely, water drops on a flat surface spread more quickly forming a film which can freeze immediately. Recently, Song and co-workers developed a micro-/nanoporous superhydrophobic surface which could efficiently control microdroplet self-removal.[52] They thought that the air sublayer in a superhydrophobic surface could provide substantial thermal insulation and thus delay the freezing process on cold superhydrophobic materials. Clearly, the induced multi-hierarchy structure will be of significance for designing new materials for applications, particularly in anti-icing, heat exchange, water harvesting, and antifogging.

3.1.3. Patterned Crystallization

New strategies for materials fabrication are of fundamental importance in the advancement of science and technology. Many methods and techniques have been used to construct nanomaterials. As an alternative to commonly used methods, exploiting patterns of contrasting wettability on 2D substrates has been demonstrated to be a simple and convenient method to prepare aligned nanomaterials.[53–55] The key for this patterning method are the carrier phases that can perform wetting or dewetting of the lyophilic/lyophobic patterned substrate which can selectively locate the carrying materials. For instance, Whitesides and co-workers demonstrated the fabrication of ordered 2D arrays of micro- and nanoparticles by using patterned self-assembled monolayer (SAM) templates. Such a pattern affords control over the density, size, and orientations of the growing crystals..[53] The crystals grown are based on inorganic salts, such as $CaCl_2$, $CuSO_4$, and KNO_3. Using a similar method, Bao and co-workers developed preparations of metallic nanorods and organic semiconducting single crystals, the orientation and assembly of which are directed by surfaces which have patterned wettability.[54] Recently, by using super-wettability surfaces to direct the preparation, we have fabricated many kinds, sizes, and orientations of patterned nanocrystals. The materials include small organic molecules, nanoparticles (Figure 4E), inorganic salts (Figure 4F), and polymers.[56] These well aligned nanostructures have potential for use in solar cells, light-emitting diodes, field-effect transistors, and highly sensitive sensors, logic computations, microcircuits and other fields.

3.1.4. Chemical Reactions

Traditional chemical reactions have been performed in test tubes, flasks, or other glass containers since the establishment of modern chemistry by Lavoisier in 1775. However, demands for the effective use of valuable reagents and solvents, precisely controlled reaction conditions, safe fabrication of explosives and the ability to integrate reactions into a digital chip require the miniaturization of chemical reaction systems. Over the past years, microreactor techniques, such as microemulsions,[57] array-based microreactors,[58] or microfluidic systems,[59] have attracted great interest since they enable the miniaturization of reactions by compartmentalizing reactions in droplets of nanoliter to microliter volumes. By restricting processes in a microscale compartment, miniature reaction system (MRS) might find promising applications, such as drug discovery, DNA analysis, and synthesis of molecules or particles, and in high-throughput analyses. Thereby, MRSs based on various principles have been gradually developed. The most effective technique utilizes superhydrophobic material to accomplish many chemical reactions, such as combination reactions, decomposition reactions, and etherification.[60,61] For example, aqueous droplets in oil provide a confined space inside the coalesced droplet reactor in which to perform a miniature reaction which requires a long reaction time and heating.[61] Beside the reactions between different aqueous droplets, some superhydrophobicity-mediated electrochemical reactions generate gold dendritic microflower arrays by using a superhydrophobic pillar-structured electrode (Figure 4G).[48] Compared with traditionally hydrophilic metal/semiconductor electrodes, this anti-wetting reaction surface allows restrictive contact between electrolyte and pillar tops owing to trapped air pockets inside structural gaps. Such a system could realize all kinds of chemical reactions know in electrochemistry.

Lei Jiang is a professor at the Institute of Chemistry, Chinese Academy of Sciences (ICCAS), and Dean of the School of Chemistry and Environment, Beihang University. He received his B.Sc. degree (1987), M.Sc. degree (1990), and Ph.D. degree (1994) from Jilin University of China (with Professor Tiejin Li). He was a postdoctoral fellow with Professor Akira Fujishima at Tokyo University, then a senior researcher at the Kanagawa Academy of Sciences and Technology under Professor Kazuhito Hashimoto. He joined ICCAS in 1999. His scientific interests are focused on bioinspired, smart, multiscale interfacial materials with super-wettability.

(A)

Rank	Field description within materials science	Core papers	Citations	Citation impact
1	Electronic properties of graphene	6	9,524	1587.3
2	Polymer solar cells	15	6,656	443.7
3	Multiferroic and magnetoelectric materials	31	6,509	210.0
4	Titanium dioxide nanotube arrays in dye-sensitized solar cells	47	5,645	120.1
5	ATRP and click chemistry in polymer synthesis	34	5,129	150.85
6	Graphene oxide sheets	16	4,815	300.9
7	Superhydrophobic surfaces	47	4,732	100.7
8	High-Tc ferromagnetism in zinc oxide diluted magnetic semiconductors	48	4,667	97.2
9	Highly selective fluorescent chemosensors	46	4,581	99.6
10	Electrospun nanofibrous scaffolds for tissue engineering	45	4,577	101.7
11	Ductile bulk metallic glasses	41	4,267	104.1
12	Single-molecule magnets	47	4,013	85.4
13	Self-assembling supramolecular nanostructured gel-phase materials	33	3,810	115.4
14	Mesoporous silica nanoparticles for drug delivery and biosensing applications	34	3,693	108.6
15	Mechanical properties of nanocrystalline metals	45	3,682	81.8
16	Discotic liquid crystals for organic semiconductors	30	3,637	121.2
17	Gold nanorods for imaging and plasmonic photothermal therapy of tumor cells	21	3,506	166.9
18	Highly ordered mesoporous polymer and carbon frameworks	25	3,362	134.5
19	Upconversion fluorescent rare-earth nanocrystals	49	3,351	68.4
20	Molecular logic circuits	47	3,315	70.5

(B)

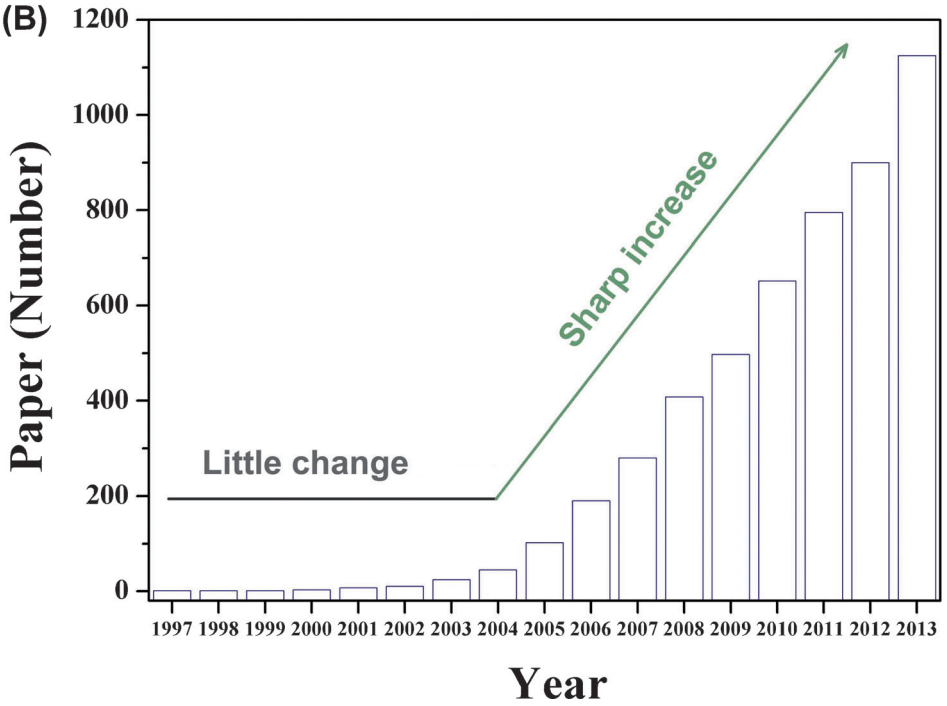

Figure 1. Super-wettability attracts interest in diverse fields. A) "Superhydrophobic surfaces" were ranked 7th in Top 20 research fronts in materials science during 2006 and 2010 from Essential Science indicators. Reproduced with permission Ref. [9]. B) Number of the papers indexed in the ISI web of science by the topic of "super-wettability".

for those in printing or related fields.[14] During the printing process, controlled wettability is one of the most important issues. Currently, the patterning of the controllable wettability of the printing-plate surface is crucial to form clear image areas and non-image areas in printing techniques based on wetting and dewetting. With the development of nanotechnology, many new micro/nano-structure processing techniques are constantly emerging, and a variety of different structures have been designed and prepared. Accordingly, a series of new techniques appeared offering special printing process. For instance, Song and co-workers developed a green printing-plate-making technology based on nanomaterials (Figure 4J; in this case green means this technique only use the changes of wettability, but not chemicals).[62–64] The detail was a specific transfer material was first printed precisely onto the superhydrophilic plate, then control of transfer materials and the interface properties between transfer-printing materials and the plate with the opposite wettability was formed on the inkjet printing plate, which could be used as the plate for printing. The oleophilic ink selectively adsorbs on the image areas, and the spreading of the ink microdroplets is well controlled. The printing plate promises to deliver printing with fine resolution, and could also be used to obtain color images through the "overprinting" technique, with high resolution. Recently, we developed an approach to precisely control patterned wettability transition (that is, the changes from hydrophobicity to hydrophilicity, and vice versa.) for liquid reprography by a photoelectric cooperative wetting process on a superhydrophobic surface of ZnO nanorod array.[65] This electro wetting is activated only at the position that is illuminated by light. Liquid will spread along the nanorod arrays but be confined by the surrounding superhydrophobic areas, indicating a type of anisotropic

3.1.5. ***Patterning and Printing***

Patterning of controllable surface wettability has attracted wide scientific attention owing to its importance in both fundamental research and practical applications, in particular

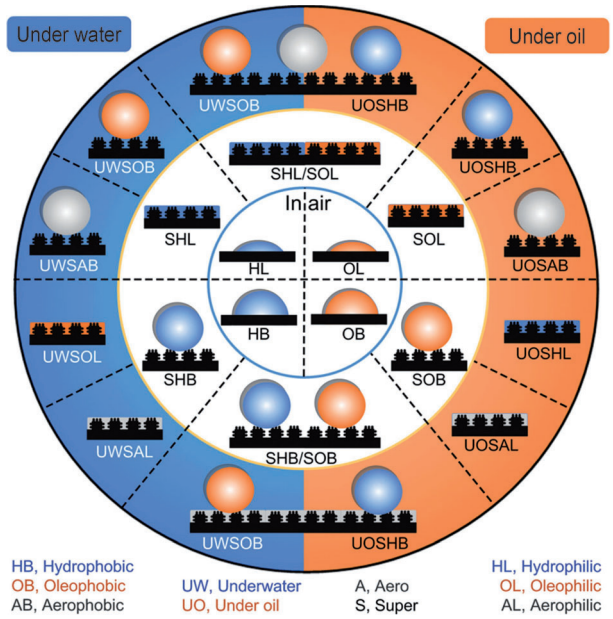

Figure 2. Super-wettability system. Inner white circle: Hydrophilicity, oleophilicity, hydrophobicity, and oleophobicity upon flat substrates in air. After introducing roughness (white ring), superhydrophilicity, superoleophilicity, superhydrophobicity, and superoleophobicity states can be generated in air. Right orange circle: Under-oil superhydrophobicity, superhydrophilicity, superaerophobicity, and superaerophilicity upon rough substrates. Left blue circle: Underwater superoleophobicity, superoleophilicity, superaerophobicity, and superaerophilicity upon rough substrates. Reproduced with permission from Ref. [10].

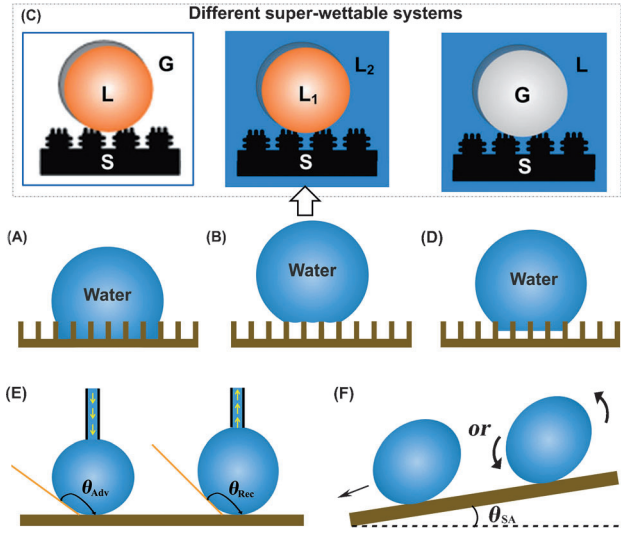

Figure 3. Effect of surface structure on the wetting behavior of solid substrates. A) Wetted contact between the liquid and the rough substrate (Wenzel's mode). B) Non-wetted contact between the liquid and the rough substrate (Cassie's mode). C) Cassie model: The extension of superhydrophobic surfaces in air, such as in SOB, UWSOB, UWSAB, UOSHB, and UOSAB states (see Figure 2).[10] S = solid phase, the L = liquid phase, and the G = gas phase. L, L_1, and L_2 can be regarded as water, polymer, liquid crystalline molecules, ionic liquids, and others. D) Intermediate state between the Wenzel and the Cassie modes. E) Advancing θ_{Adv} and receding contact angle θ_{Rec}. F) Tilt angle, that is, the so-called roll-off angle or sliding angle θ_{SA}.

wetting. Based on this strategy, we successfully performed the liquid reprography process, and the wetting error of the system could be well controlled, making it a suitable strategy for liquid reprography. The controllable surface wettability of the printing materials and the combination of different printing techniques for creating patterned surface wettability will play a more important role in digital and green printing in the future.

3.2. Application of Three-Dimensional Super-Wettability Surfaces

3.2.1. Oil/Water Separation

In addition to two dimensional wettability surfaces, three-dimensional super-wettability surfaces also have important applications, particularly in the treatment of oily wastewater. To date, various technologies, such as gravity separation, oil-absorbing materials, coagulation, and flocculation have been used to separate oil/water mixtures.[66–68] However, these methods are either ineffective in treating emulsified oil/water mixtures, or to demulsify the emulsions require the application of an electric field or the addition of chemicals, which usually involves energy consumption and secondary pollution.[69,70]

Superoleophilic materials have gained attention as a result of their surface energies being similar to that of the oil drops, which suggests these could be used in oil/water separation. We first reported an oil/water separation system that involved coating polytetrafluoroethylene (PTFE) onto a stainless mesh by a spray-and-dry method.[50,71] The prepared membrane shows superoleophilicity, and a diesel oil droplet could spread and permeate the mesh film thoroughly and quickly. Thus a mixture of diesel oil and water can be successfully separated using this mesh film (Figure 4I). Later, Wu, Cao et al. reported a carbon-nanotube sponge with high structural flexibility, robustness, and wettability to organics.[72] Such a sponge can absorb a wide range of solvents and oils with excellent selectivity, recyclability, and absorption capacities. Recently, we developed a novel superhydrophilic and underwater superoleophobic poly(acrylic acid)-grafted poly(vinylidene fluoride)(PVDF) filtration membrane using a salt-induced phase-inversion approach.[73] Such a membrane could separate both surfactant-free and surfactant-stabilized oil-in-water emulsions under either a small applied pressure (<0.3 bar) or gravity, with high separation efficiency and high flux. Furthermore, various filtration membranes with super-wettability have also been developed by blending and surface-modifying techniques, and most of them have been used in oil/water separation with high flux, have antifouling performance, and are unaffected by high transmembrane pressure.

3.2.2. Biological Applications

Surface properties, including composition, topography, charge, and wettability, are of great importance in both fundamental research and practical applications. Although these factors usually work together to have a cooperation effect, surface wettability, which usually acts as an integrated

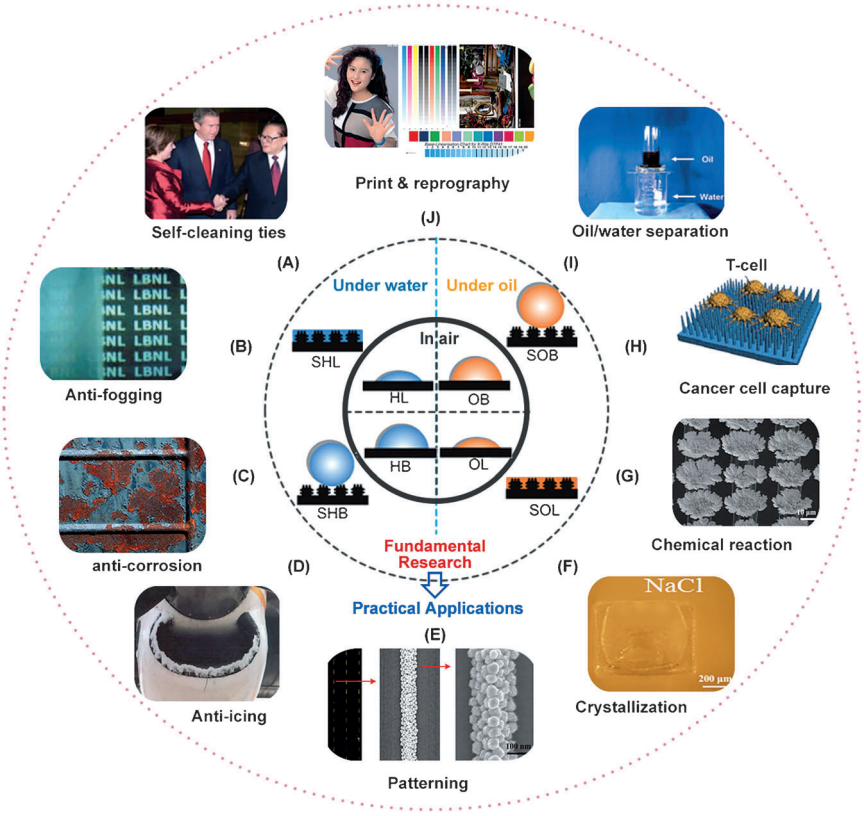

Figure 4. Super-wettability systems, from fundamental research to practical applications. The middle part: hydrophilicity, oleophilicity, hydrophobicity, and oleophobicity upon flat substrates in air. After introducing roughness, superhydrophilicity, superoleophilicity, superhydrophobicity, and superoleophobicity states can be generated in air, water, and oil systems. Representative applications of super-wettability surfaces. A) superamphiphobic textiles show an excellent self-cleaning property. Reproduced with permission from Ref. [24]. B) Anti-fogging, the superhydrophilic coatings can spread the condensed water droplets quickly to form a thin sheet-like film and dramatically suppress the fogging behavior. Reproduced with permission from Ref. [45]. C) For anti-corrosion, air trapped between the superhydrophobic coating and solution can provide an effective barrier to prevent the migration of corrosive ions. D) Anti-icing, the superhydrophobic surfaces can delay and reduce the accumulation/adhesion of wet snow, ice, and frost. E) Patterning, wafer-scale array of 1D assemblies of silver nanoparticles with precise orientation and position, prepared through the sandwich-shaped assembly strategy on superhydrophobic surfaces. Reproduced with permission from Ref. [46]. F) For crystallization: patterned NaCl crystal arrays are generated on high-adhesion superhydrophobic substrates. Reproduced with permission from Ref. [47]; G) For chemical reactions, Au architectures can be formed using a superhydrophobic pillar structured surface. Reproduced with permission from Ref. [48]; H) Cancer-cell capture, local topographic interactions between superhydrophilic rough surfaces and cell extensions have the ability to capture cancer cells. Reproduced with permission from Ref. [49]; I) For oil/water separation, the combination of superhydrophobicity and superoleophilicity can lead to functional coatings which have the capability to separate oil/water mixtures. Reproduced with permission from Ref. [50]; J) For print and reprography, using a green printing-plate-making technology colorful images could also be obtained through "overprinting" with fine resolution.

factor, is one of the most important parameters affecting their uses in biological applications, such as enhanced cell adhesion, controlled cell adhesion/detachment, and protein adsorption. Adhesion is one of the fundamental cell activities. During the past few decades, several three-dimensional surface materials have been designed for regulating cell adhesion. They show enhanced cell adhesion when compared with the corresponding two-dimensional biointerfaces. For example, Lampin et al. observed the enhancement of cell adhesion in relation to the degree of roughness of a poly(methylmethacrylate) (PMMA) surface a result of the corresponding enhanced surface hydrophobicity which favored the adsorption of adhesive proteins.[74] We previously developed a kind of blood-compatible nanostructured superhydrophobic surface by dip-coating fluorinated poly(-carbonate urethane) onto aligned carbon nanotube films.[75] Recently, we developed a pH-value and glucose dual-responsive surface by grafting poly(acrylamidophenylboronic acid) (poly-AAPBA) brushes onto aligned silicon nanowire (SiNW) arrays.[76] Such a surface can reversibly capture and release targeted cancer cells by precisely controlling pH value and the glucose concentration, exhibiting dual-responsive AND logic, thus this dual-responsive surface can significantly impact biomedical and biological applications including cell-based diagnostics and in vivo drug delivery. At the same time, a thermoresponsive nanostructured surface-poly(N-isopropylacrylamide) (PNIPAAm) coated silicon nanopillar array that can reversibly capture and release targeted cancer cells by combining hydrophobic interactions with topographic interactions has been developed. (Figure 4H).[49] Such a system provides a new method in the design of bio-interfacial materials and offers a general strategy to fabricate next-generation artificial smart surfaces, which would be useful for reversible capture/release of targeted cells, bacteria, and viruses.[77]

In addition to the above mentioned 3D interfacial materials, slippery liquid-infused porous surfaces are another important class of novel and functional interfacial material which could be used in marine antibiofouling,[78] anti-icing,[79] self-repairing,[80] and antibacterial applications.[81]

3.3. Application of One-Dimensional Super-Wettability Surfaces

3.3.1. Water Collection with Biomimetic-Based Fiber

Efficient water collection from a humid atmosphere is critical for organisms living in water-limited areas. One striking example is the Namib desert Stenocara beetle,[5] which uses the patterned wettability surfaces on its back to collect water from fog. In addition to such two-dimensional surfaces in living systems, one-dimensional wettability surfa-

ces are now drawing more and more attention. One good example is spider silks which possess not only outstanding strength and toughness but also the ability to collect water from humid air (Figure 5A). Our recent study showed that the water-collecting ability of capture silk of the *cribellate* spider is a result of its unique arrangement of periodic spindle-knots and the joints, both of which result in surface energy gradients and Laplace pressure between the spindle-knots and the joints (Figure 5B).[7] Inspired by this finding, we designed and fabricated artificial fibers which mimic the structural features of this spider silk and exhibit its directional water-collecting ability (Figure 5C).[82,83] This work could help in the design of functional fibers for use in water collection (Figure 5D) and for filtering liquid aerosols in manufacturing processes.

In addition to spider silks, cacti are well-known for their capability to thrive in the extreme water-shortage found in deserts (Figure 5E). The cactus can collect and transport water droplets by its efficient fog collection system.[84] This unique system is composed of well-distributed clusters of conical spines and trichomes on the cactus stem (Figure 5F). Each spine contains three integrated parts that have different roles in the process of fog collection. The gradient of the Laplace pressure, the gradient of the surface free energy, and multi-function integration endow the cactus with an efficient fog collection system. Investigation of the structure–function relationship in this system may help us to design novel materials and devices to collect water from fog with high efficiencies (Figure 5G). Inspired by the water collecting of cactus, we developed a novel and efficient continuous fog collector (Figure 5H).[85,86] Cactus spine-like conical micro-tip arrays were fabricated through a modified magnetic particle-assisted molding (MPAM) method using polydimethylsiloxane (PDMS) and cobalt magnetic particles (MPs) under an external magnetic field. Such a system can spontaneously and continuously collect, transport, and preserve the fog water. Thus this fog collector has promise for application in regions in which drinking water is scarce, which provides a potential avenue to alleviate the growing global water crisis.[13]

3.3.2. Micro-Sized Oil Collection with Biomimetic-Based Fiber

Although great success has been achieved in oil/water separation by using three-dimensional super-wettability surfaces, these surfaces are not collecting micro-sized oil droplet (this is a problem because the micro-sized oil droplets not only contaminate the environment but also lost the non-renewable resource). Also, achieving a high continuity or high throughput remains a challenge. Because micro-sized oil droplets in water are similar to micro-sized water droplets in air, we can move the cactus-inspired system underwater. Inspired by the directional water collection on cactus spines, a novel "artificial cactus under water" was developed to directionally collect micro-sized oil droplets from oil/water mixtures (Figure 5I).[87] The oleophilic conical needle structure developed can successfully separate micron-sized oil droplets from the oil/water mixture and can drive the droplets towards their base, thus the continuous and effective collection of micron-sized oil droplets from water is achieved. Clearly, although much progress toward fabrication and application of one-dimensional materials used in air, water, and material surfaces has been achieved, there are numerous challenges and opportunities ahead for its development in other super-wettability systems (Figure 2). Therefore, more applications related to the liquid- or gas-collector and transportation systems need to be designed and fabricated for the future.

3.3.3. Liquid Transfer on the Outer Surfaces of One-Dimensional Materials

Droplets sitting on surfaces which have different wetting states will present different contact areas, contact angles, and contact angle hysteresis. Hence, it is possible to control droplet motion and liquid transfer by tuning surface wettability. A Chinese brush, which is made of a bundle of freshly emergent animal hairs (that is, hairs that have not been previously cut so the original tip is still intact) in a quasi-parallel arrangement (Figure 5J), allows the manipulation of low-viscosity liquid ink in a controlled manner: high-mass ink loading and steady, uniform, and continuous ink transfer onto the substrate. However, the mechanism responsible for the liquid transfer, specifically the critical role of the freshly emergent hairs (FE-hairs), has yet to be rationalized. Recently, we reported the mechanism by which the Chinese brush functions, which is an integrated system which allows the dynamic balance of large mass liquid and consequent controllability of liquid transfer.[88] This unique liquid manipulation behavior is attributable to the anisotropic multi-scale structural feature of FE-hairs (Figure 5K). Meanwhile, inspired by the fascinating ability of FE-hairs to offer controllable liquid transfer, a model device has been designed and fabricated by us in which two FE-hairs were fixed in parallel and were connected with an artificial-made liquid reservoir for continuous liquid supply (Figure 5L). Upon deforming the hair tips, the balance of the liquid that was held by this model device would be perturbed and the liquid would be steadily, uniformly and continuously transferred onto substrates in a controllable manner. Such a model device enables one-dimensional micro-lines to be deposited on diverse substrates through the direct writing of liquid-phase materials and thus provides a new simple alternative for the preparation micro-lines.

3.4. Application of Biomimetic-Based Nanochannel or Nanopore

Water's behavior in confined spaces is quite different from that in the bulk, and plays an important role in a wide variety of life activities, such as water transport,[89] protein folding,[90] and gating of ion channels.[91–93] The transport of water molecules through these biological nanopores is of great importance in many physiological processes. Up to now, different techniques including simulation and artificial nanochannels have been used to study biological ion channels (see middle part in Figure 6).[94] To develop a more concise model for confined water, researchers study the wetting behavior of water in artificial nanopores.[95,96] Based on molecular dynam-

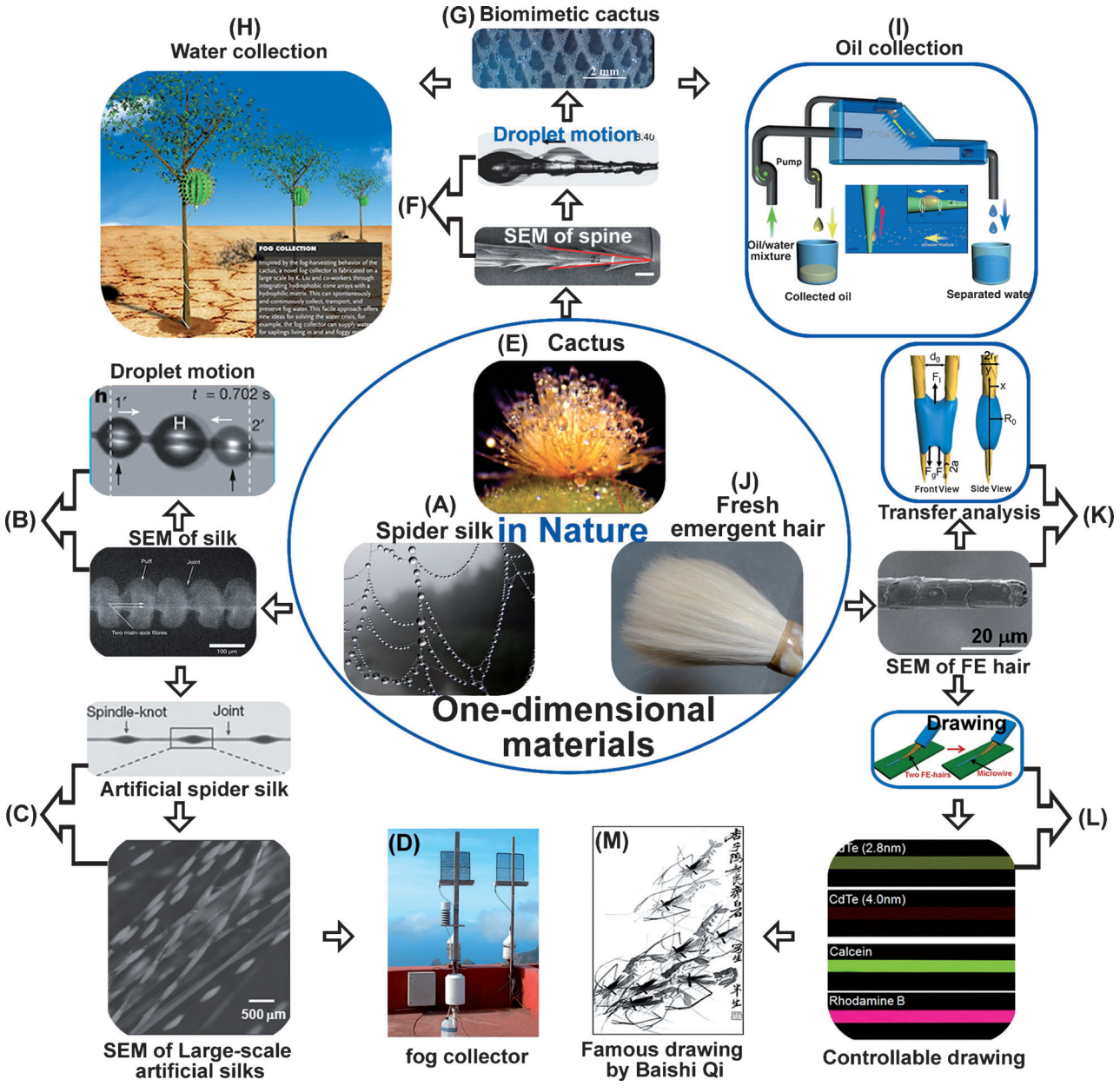

Figure 5. Super-wettability-based controllable droplet motion and collection. A) Optical image and B) environmental SEM observation of a spider silk with periodic spindle-knots, which can drive the water droplet movement in a controlled direction. Reproduced with permission from Ref. [7]; C,D) Optical image of artificial spider silks and their application in fog collection. E) An *O. microdasys* stem consisting of sharp spines and trichomes. Reproduced with permission from Ref. [84]. F) SEM image of a spine from the *O. microdasys* stem and the directional droplet motion along the spine. The smaller droplets first condensed randomly upon the spine, then coalesced and moved towards the wider part as a result of the Laplace pressure. G) Optical image of artificial cactus used for water collection (H). Reproduced with permission from Ref. [86]. I) Schematic representation of the oil collection process. Micron-sized oil droplets deposit on the needle. The collected oil droplet grows and is then driven upwards. Reproduced with permission from Ref. [87]. J) Optical image of fresh emergent-hair (FE-hair). K) SEM images of a single FE-hair and the mechanism of the dynamic balance of a drop on "two parallel hairs". L) Direct writing of micro-lines by a simple template-free printing model device based on "two parallel FE-hairs". Reproduced with permission from Ref. [88]. M) A famous drawing made by Baishi Qi, whose drawings have been finished by Chinese brush made by FE-hair.

ics simulations, Hummer et al. reported pulse-like transmission of water through a nonpolar carbon nanotube (see middle part in Figure 6).[97] They found the transmission bursts result from the tight hydrogen-bonding network inside the tube which ensures that density fluctuations in the surrounding bath lead to concerted and rapid motion along the tube axis. With the development of experimental and computational methods, rapid progress has been made in the study of water transportation across artificial nanopores, which has important biological implications and shows promising applications in designing novel molecular sensors, energy conversion system, and nanofluidic devices.

3.4.1. *Biomimetic Nanochannels with Tunable Wettability*

Biological nanochannels can use their unique protein complex to selectively transport ions. Inspired by living systems, researchers have fabricated a series of smart nanochannels with tunable wettability (Figure 6B). We and others attached thermo-responsive polymer brushes (poly(N-isopropylacrylamide), PNIPAAm) onto the polyethylene terephthalate (PET) nanopores to control the wettability.[100,105] Such a system could be used as a thermally driven ionic gate controlling the ion transportation through the nanopores. Below the lower critical solution temperature (LCST), the PNIPAAm brushes are hydrophilic and in a swollen state; above the LCST they are hydrophobic and in a collapsed state. With controlled temperature change, the PNIPAAm-modified nanopore switches from a low-conducting state to a high-conducting state as a temperature-triggered ionic gate. Besides the thermo-controllable ionic gate, Smirnov et al. and our group developed photo-induced ionic gates by attaching photochromic spiropyran isomers to the inner surface of a nanopore.[101,106] With visible irradiation, the spiropyran is thermally stable and exhibits a hydrophobic form, so that the nanopores are unwetted by an aqueous solution. Under UV irradiation, the spiropyran converts into a more polar merocyanine form, and the nanopores allow the permeation of water. Meanwhile, the nanofluidic transport induced by the

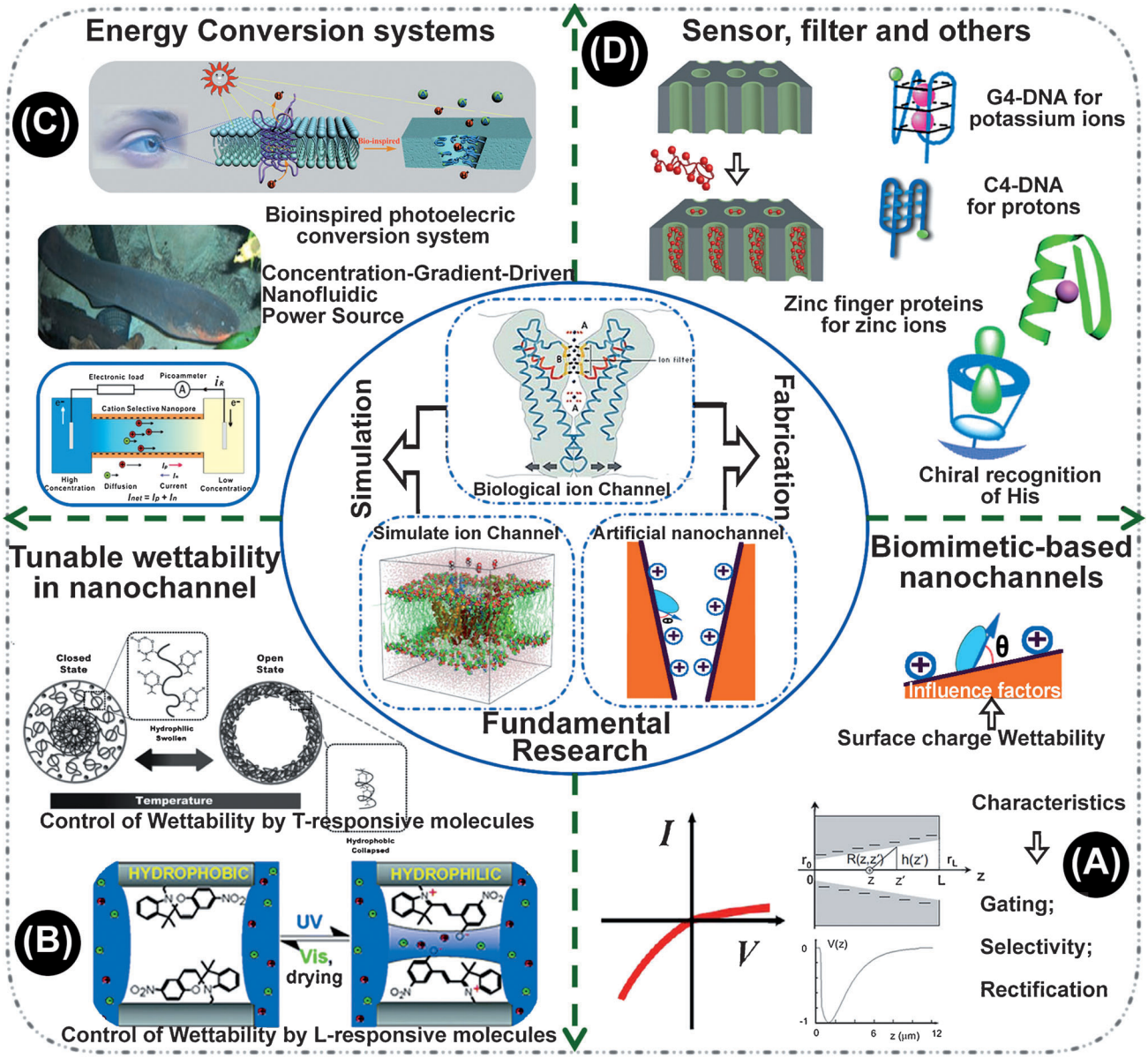

Figure 6. Biomimetic-based nanochannel from fundamental researches to practical applications. The middle part: Fundamental research of biological nanochannels, simulate nanochannels and the artificial nanochannels. Reproduced with permission from Ref. [98]; A) Basic researches of biomimetic nanochannels. Reproduced with permission from Ref. [99]; B) Biomimetic nanochannels with tunable wettability. Reproduced with permission from Ref. [100,101]; C) Bioinspired energy conversion systems. Reproduced with permission from Ref. [102,103]; D) Biomimetic nanochannels used in filtration and sensing systems. Reproduced with permission from Ref. [104].

axial wettability gradient has also been shown by modifying PNIPAAm and poly (acrylic acid)PAA on the opposing chambers of an hourglass-shaped single-nanopore.[107] The wettability of the attached molecular layer on the pore wall can be regulated by changing the temperature and pH value. This wettability difference results in distinct ionic rectifying properties compared with the unmodified nanopores. Therefore, wettability-controllable nanochannels can help us to understand the characteristics of confined water or of ion transport in nanoscale environments.[108]

3.4.2. Energy-Conversion System

The global energy demand is growing constantly. Many different materials and techniques are used for constructing energy-conversion systems. Recently, much effort has been focused on constructing the biomimetic nanofluidic energy conversion devices. For example, Dekker and co-workers first reported electrokinetic energy conversion with solid-state nanochannels.[109] Based on artificial nanochannels, we and others demonstrated some energy-conversion systems whose inspiration come from retina[102,110] and electric eels (Figure 6C).[103,111] Recently, we demonstrated an integrated two-dimensional nanofluidic generator with a layered graphene hydrogel membrane (GHM).[112] In wet conditions, two-dimensional nanocapillaries are formed between adjacent graphene sheets giving a large-scale interconnected two-dimensional nanofluidic network. Because the two-dimensional graphene hydrogel membrane is negatively charged it allows counter-ions to permeate and excludes co-ions. Once electrolytes flow from the GHM, driven by an external mechanical force, an electrokinetic phenomenon occurs. Based on this principle, the integrated two-dimensional nanofluidic generators convert hydraulic motion into a streaming ionic current. Such a two-dimensional nanofluidic generator would be used for harvesting electricity from footsteps or a stream of body fluid, or monitoring the heartbeat. Very recently, we developed a ionic diode membrane-based nanofluidic device for harvesting electric power from a salinity gradient.[111] The meso-/macroporous membrane rectifies the ionic current with a high ratio of approximately 450 and keeps on rectifying in high-concentration electrolytes, even in saturated solution. By mixing artificial seawater and river water through the IDM, a high power density of up to 3.46 $W m^{-2}$ is generated, which outperforms some commercial ion-exchange membranes. Such an asymmetric structure macroscopic nanofluidic system may have potential application for sustainable power generation, water purification, and desalination.

3.4.3. Biomimetic Nanochannel-Based Sensor

The sensing of individual molecules has drawn great interest within modern biochemistry, biophysics, and chemistry. Detecting individual molecules can also lead to the development of next-generation bioanalytical and diagnostic tools. In nanopore sensing, individual molecules pass through a nanoscale pore leading to detectable changes in the ionic current in the pore. The range of analytes that can be detected with nanopores now spans small molecules,[113] organic polymers,[114] peptides, enzymes, proteins,[115] and biomolecular complexes. Indeed, nanopore recording has developed from a simple sensing tool into a general platform technology which enables the examination of the physicochemistry, biophysics, and chemistry of individual molecules. Inspired by ion-selective biological channels, attempts were made to prepare nanopores that are selective for simple inorganic ions, such as potassium,[116] zinc,[117] mercury,[118] and silver ions (Figure 6D).[119] The mechanisms by which solid-state nanopores can achieve ion selectivity are certainly different to those of biological channels because the inner diameter of biological channels is less than 1 nm. However, a simple way of attaining ionic selectivity in solid-state nanopores involves the introduction of stimuli-responsive molecules, such as G-quadruplex DNA to detect potassium, zinc responsive peptide to detect zinc, and thymine–thymine base DNA to detect mercury. Besides inorganic ions, chiral-molecule recognition has also been realized by attaching a chiral ligand onto the synthetic nanochannels. For example, we developed a chiral analysis based on enantioselective recognition with β-cyclodextrin-modified single conical nanopores, which detects enantiomer-specific L-histidine by monitoring the rectified ionic current.[120] Clearly, if appropriate receptors were modified, these nanochannel systems may show applications in many fields, such as drug detection and the analysis of the real samples.

3.4.4. Other Applications

Smart nanopore/nanochannels with super-wettability could also be used as molecular filters. Separation of small organic molecules and large biomolecules is of great importance in pharmaceutical and biological applications. Molecular recognition with a nanoporous membrane is particularly attractive because of the advantages associated with molecular interactions in confined spaces. Traditional separations simply use a difference in the size of analytes relative to pore size in the membrane. To improve the separation properties of the size-fixed nanoporous membranes, it is necessary to functionalize them. For example, Thayumanavan and co-workers developed a simple approach to functionalize nanopores, and these modified nanopores could be used separate small molecules which transported through the nanopores based on their size and/or electrostatics (Figure 6D).[104]

4. Summary and Outlook

Although the topic of super-wettability has changed dramatically in the last decade and will probably change even more in the next decade, its fundamental character remains the same. Super-wettability is the most fundamental property of a solid surface and is closely related to everything in nature. This property goes beyond superhydrophobicity in air and applies to many systems on different surfaces including under water and under oil etc. systems(Figure 3), as most of the results remain on a theoretical basis, many problems need to be resolved before practical applications

are possible. Researchers need to combine diverse super-wettability features into one surface, such as catalytic electrodes or direct inkjet computer-to-plate printing techniques. Only in this way, will unexpected and yet unimagined functions be discovered. The developed functions would thus pave the way for applying super-wettability surfaces in practical applications which could help to guide the future research and bridge the gap between fundamental research and practical applications.

As the applications for super-wettability surfaces involve many fields, such as biology, chemistry, physics, material and engineering, intensive collaboration from various disciplines is necessary to vigorously push the study of super-wettability forward, so as to bring benefits to society. What the expected developments will be in the next years is, of course, hard to say, however it can be predicted easily that the super-wettability will remain a hot topic and will be used extensively. The rate of development in super-wettability-based materials and devices in the fields surrounding it is rapid and there is, fortunately, there is no doubt that there will be unexpected developments, and super-wettability systems will find use in environmental protection, energy, green industry, and many other important domains.

This work was supported by the National Research Fund for Fundamental Key Projects (2011CB935703, 2011CB935704), the National Natural Science Foundation (21171171, 21434003, 21431009, 21201170, 91127025, 20920102036, 21421061), and the Key Research Program of the Chinese Academy of Sciences (KJZD-EW-M01)and (KJZD-EW-M03).

Received: October 9, 2014
Published online: January 22, 2015

[1] T. Young, *Philos. Trans. R. Soc. London* **1805**, *95*, 65.
[2] H. Ollivier, *Ann. Chim. Phys.* **1907**, *10*, 229 – 288.
[3] W. Barthlott, C. Neinhuis, *Planta* **1997**, *202*, 1 – 8.
[4] L. Feng, S. H. Li, Y. S. Li, H. J. Li, L. J. Zhang, J. Zhai, Y. L. Song, B. Q. Liu, L. Jiang, D. B. Zhu, *Adv. Mater.* **2002**, *14*, 1857 – 1860.
[5] A. R. Parker, C. R. Lawrence, *Nature* **2001**, *414*, 33 – 34.
[6] X. F. Gao, L. Jiang, *Nature* **2004**, *432*, 36 – 36.
[7] Y. Zheng, H. Bai, Z. Huang, X. Tian, F. Q. Nie, Y. Zhao, J. Zhai, L. Jiang, *Nature* **2010**, *463*, 640 – 643.
[8] M. J. Liu, S. T. Wang, Z. X. Wei, Y. L. Song, L. Jiang, *Adv. Mater.* **2009**, *21*, 665 – 669.
[9] J. Adams, D. Pendlebury, Global Research Report: Materials Science and Technology, Thomson Reuters ScienceWatch, **2011**, 1 – 16.
[10] Y. Tian, B. Su, L. Jiang, *Adv. Mater.* **2014**, *26*, 6872 – 6897.
[11] X. Yao, Y. L. Song, L. Jiang, *Adv. Mater.* **2011**, *23*, 719 – 734.
[12] H. Bai, J. Ju, Y. M. Zheng, L. Jiang, *Adv. Mater.* **2012**, *24*, 2786 – 2791.
[13] J. Ju, Y. Zheng, L. Jiang, *Acc. Chem. Res.* **2014**, *47*, 2342 – 2352.
[14] D. Tian, Y. Song, L. Jiang, *Chem. Soc. Rev.* **2013**, *42*, 5184 – 5209.
[15] K. S. Liu, X. Yao, L. Jiang, *Chem. Soc. Rev.* **2010**, *39*, 3240 – 3255.
[16] T. L. Sun, L. Feng, X. F. Gao, L. Jiang, *Acc. Chem. Res.* **2005**, *38*, 644 – 652.
[17] X. J. Feng, L. Jiang, *Adv. Mater.* **2006**, *18*, 3063 – 3078.
[18] R. N. Wenzel, *Ind. Eng. Chem.* **1936**, *28*, 988 – 994.
[19] A. B. D. Cassie, S. Baxter, *Trans. Faraday Soc.* **1944**, *40*, 546 – 551.
[20] A. Lafuma, D. Quere, *Nat. Mater.* **2003**, *2*, 457 – 460.
[21] Y. Tian, L. Jiang, *Nat. Mater.* **2013**, *12*, 291 – 292.
[22] E. A. Vogler, *Adv. Colloid Interface Sci.* **1998**, *74*, 69 – 117.
[23] L. Gao, T. J. McCarthy, *Langmuir* **2006**, *22*, 5998 – 6000.
[24] Editorial, *Nat. Mater.* **2005**, *4*, 355 – 355.
[25] A. Nakajima, A. Fujishima, K. Hashimoto, T. Watanabe, *Adv. Mater.* **1999**, *11*, 1365 – 1368.
[26] H. Yabu, M. Shimomura, *Chem. Mater.* **2005**, *17*, 5231 – 5234.
[27] J. Bravo, L. Zhai, Z. Wu, R. E. Cohen, M. F. Rubner, *Langmuir* **2007**, *23*, 7293 – 7298.
[28] W.-L. Min, B. Jiang, P. Jiang, *Adv. Mater.* **2008**, *20*, 3914 – 3918.
[29] S. T. Wang, L. Feng, L. Jiang, *Adv. Mater.* **2006**, *18*, 767 – 770.
[30] E. Hermelin, J. Petitjean, J.-C. Lacroix, K. I. Chane-Ching, J. Tanguy, P.-C. Lacaze, *Chem. Mater.* **2008**, *20*, 4447 – 4456.
[31] X. Liu, S. Wang, *Chem. Soc. Rev.* **2014**, *43*, 2385 – 2401.
[32] J. Vince, B. Orel, A. Vilčnik, M. Fir, A. Šurca Vuk, V. Jovanovski, B. Simončič, *Langmuir* **2006**, *22*, 6489 – 6497.
[33] M. Barletta, S. Vesco, V. Tagliaferri, *Colloids Surf. B* **2014**, *120*, 71 – 80.
[34] H. J. Lee, J. Kim, C. H. Park, *Text. Res. J.* **2014**, *84*, 267 – 278.
[35] Y. D. Kim, J.-H. Shin, J.-Y. Cho, H.-J. Choi, H. Lee, *Phys. Status Solidi A* **2014**, *211*, 1822 – 1827.
[36] Y. Paz, Z. Luo, L. Rabenberg, A. Heller, *J. Mater. Res.* **1995**, *10*, 2842 – 2848.
[37] N. P. Mellott, C. Durucan, C. G. Pantano, M. Guglielmi, *Thin Solid Films* **2006**, *502*, 112 – 120.
[38] X. Deng, L. Mammen, H.-J. Butt, D. Vollmer, *Science* **2012**, *335*, 67 – 70.
[39] S. Pan, A. K. Kota, J. M. Mabry, A. Tuteja, *J. Am. Chem. Soc.* **2013**, *135*, 578 – 581.
[40] H. F. Meng, S. T. Wang, J. M. Xi, Z. Y. Tang, L. Jiang, *J. Phys. Chem. C* **2008**, *112*, 11454 – 11458.
[41] J. M. Xi, L. Feng, L. Jiang, *Appl. Phys. Lett.* **2008**, *92*, 053102.
[42] H. F. Hoefnagels, D. Wu, G. de With, W. Ming, *Langmuir* **2007**, *23*, 13158 – 13163.
[43] A. Vilčnik, I. Jerman, A. Šurca Vuk, M. Koželj, B. Orel, B. Tomšič, B. Simončič, J. Kovač, *Langmuir* **2009**, *25*, 5869 – 5880.
[44] D. Pasqui, R. Barbucci, *J. Photochem. Photobiol. A* **2014**, *274*, 1 – 6.
[45] R. Wang, K. Hashimoto, A. Fujishima, M. Chikuni, E. Kojima, A. Kitamura, M. Shimohigoshi, T. Watanabe, *Nature* **1997**, *388*, 431 – 432.
[46] B. Su, C. Zhang, S. Chen, X. Zhang, L. Chen, Y. Wu, Y. Nie, X. Kan, Y. Song, L. Jiang, *Adv. Mater.* **2014**, *26*, 2501 – 2507.
[47] B. Su, S. Wang, J. Ma, Y. Song, L. Jiang, *Adv. Funct. Mater.* **2011**, *21*, 3297 – 3307.
[48] Y. Wu, K. Liu, B. Su, L. Jiang, *Adv. Mater.* **2014**, *26*, 1124 – 1128.
[49] L. Chen, X. L. Liu, B. Su, J. Li, L. Jiang, D. Han, S. T. Wang, *Adv. Mater.* **2011**, *23*, 4376 – 4380.
[50] Z. X. Xue, S. T. Wang, L. Lin, L. Chen, M. J. Liu, L. Feng, L. Jiang, *Adv. Mater.* **2011**, *23*, 4270 – 4273.
[51] P. Tourkine, M. Le Merrer, D. Quéré, *Langmuir* **2009**, *25*, 7214 – 7216.
[52] M. He, Q. Zhang, X. Zeng, D. Cui, J. Chen, H. Li, J. Wang, Y. Song, *Adv. Mater.* **2013**, *25*, 2291 – 2295.
[53] J. Aizenberg, A. J. Black, G. M. Whitesides, *Nature* **1999**, *398*, 495 – 498.
[54] S. Liu, J. B. H. Tok, J. Locklin, Z. Bao, *Small* **2006**, *2*, 1448 – 1453.
[55] Z.-Z. Gu, A. Fujishima, O. Sato, *Angew. Chem. Int. Ed.* **2002**, *41*, 2067 – 2070; *Angew. Chem.* **2002**, *114*, 2171 – 2174.
[56] B. Su, Y. Wu, L. Jiang, *Chem. Soc. Rev.* **2012**, *41*, 7832 – 7856.

[57] M. A. López-Quintela, C. Tojo, M. C. Blanco, L. G. Rio, J. R. Leis, *Curr. Opin. Colloid Interface Sci.* **2004**, *9*, 264 – 278.
[58] G. A. Gross, H. Wurziger, G. Schlingloff, A. Schober, *QSAR Comb. Sci.* **2006**, *25*, 1055 – 1062.
[59] A. J. deMello, *Nature* **2006**, *442*, 394 – 402.
[60] B. Su, S. T. Wang, Y. L. Song, L. Jiang, *Nano Res.* **2011**, *4*, 266 – 273.
[61] B. Su, S. T. Wang, Y. L. Song, L. Jiang, *Soft Matter* **2012**, *8*, 631 – 635.
[62] Y. L. Song, *Bull. Chin. Acad. Sci.* **2011**, *25*, 52.
[63] H. H. Zhou, Y. L. Song, *Adv. Mater. Res.* **2011**, *174*, 447 – 449.
[64] Y. L. Song, K. Xiao, J. G. Yang, Y. G. Liu, CN Patent 201020581058.201020581057, **2010**.
[65] D. L. Tian, Q. W. Chen, F. Q. Nie, J. J. Xu, Y. L. Song, L. Jiang, *Adv. Mater.* **2009**, *21*, 3744 – 3749.
[66] M. Cheryan, N. Rajagopalan, *J. Membr. Sci.* **1998**, *151*, 13 – 28.
[67] A. A. Al-Shamrania, A. Jamesa, H. Xiao, *Water Resour.* **2002**, *29*, 1503 – 1512.
[68] Y. Zhu, D. Wang, L. Jiang, J. Jin, *Npg Asia Mater.* **2014**, *6*, e101.
[69] G. Kwon, A. K. Kota, Y. X. Li, A. Sohani, J. M. Mabry, A. Tuteja, *Adv. Mater.* **2012**, *24*, 3666 – 3671.
[70] T. Ichikawa, *Colloids Surf. A* **2007**, *302*, 581 – 586.
[71] L. Feng, Z. Y. Zhang, Z. H. Mai, Y. M. Ma, B. Q. Liu, L. Jiang, D. B. Zhu, *Angew. Chem. Int. Ed.* **2004**, *43*, 2012 – 2014; *Angew. Chem.* **2004**, *116*, 2046 – 2048.
[72] X. Gui, J. Wei, K. Wang, A. Cao, H. Zhu, Y. Jia, Q. Shu, D. Wu, *Adv. Mater.* **2010**, *22*, 617 – 621.
[73] W. Zhang, Z. Shi, F. Zhang, X. Liu, J. Jin, L. Jiang, *Adv. Mater.* **2013**, *25*, 2071 – 2076.
[74] M. Lampin, R. Warocquier-Clerout, C. Legrs, M. Degrange, M. F. Sigot-Luizard, *J. Biomed. Mater. Res.* **1997**, *36*, 99 – 108.
[75] T. L. Sun, H. Tan, D. Han, Q. Fu, L. Jiang, *Small* **2005**, *1*, 959 – 963.
[76] H. Liu, Y. Li, K. Sun, J. Fan, P. Zhang, J. Meng, S. Wang, L. Jiang, *J. Am. Chem. Soc.* **2013**, *135*, 7603 – 7609.
[77] H. Liu, X. Liu, J. Meng, P. Zhang, G. Yang, B. Su, K. Sun, L. Chen, D. Han, S. Wang, L. Jiang, *Adv. Mater.* **2013**, *25*, 922 – 927.
[78] L. Xiao, J. Li, S. Mieszkin, A. Di Fino, A. S. Clare, M. E. Callow, J. A. Callow, M. Grunze, A. Rosenhahn, P. A. Levkin, *ACS Appl. Mater. Interfaces* **2013**, *5*, 10074 – 10080.
[79] P. W. Wilson, W. Lu, H. Xu, P. Kim, M. J. Kreder, J. Alvarenga, J. Aizenberg, *Phys. Chem. Chem. Phys.* **2013**, *15*, 581 – 585.
[80] T.-S. Wong, S. H. Kang, S. K. Y. Tang, E. J. Smythe, B. D. Hatton, A. Grinthal, J. Aizenberg, *Nature* **2011**, *477*, 443 – 447.
[81] J. Li, T. Kleintschek, A. Rieder, Y. Cheng, T. Baumbach, U. Obst, T. Schwartz, P. A. Levkin, *ACS Appl. Mater. Interfaces* **2013**, *5*, 6704 – 6711.
[82] H. Bai, J. Ju, R. Sun, Y. Chen, Y. Zheng, L. Jiang, *Adv. Mater.* **2011**, *23*, 3708 – 3711.
[83] H. Bai, R. Sun, J. Ju, X. Yao, Y. Zheng, L. Jiang, *Small* **2011**, *7*, 3429 – 3433.
[84] J. Ju, H. Bai, Y. Zheng, T. Zhao, R. Fang, L. Jiang, *Nat. Commun.* **2012**, *3*, 1247
[85] J. Ju, K. Xiao, X. Yao, H. Bai, L. Jiang, *Adv. Mater.* **2013**, *25*, 5937 – 5942.
[86] M. Cao, J. Ju, K. Li, S. Dou, K. Liu, L. Jiang, *Adv. Funct. Mater.* **2014**, *24*, 3235 – 3240.
[87] K. Li, J. Ju, Z. Xue, J. Ma, L. Feng, S. Gao, L. Jiang, *Nat. Commun.* **2013**, *4*, 2276
[88] Q. Wang, B. Su, H. Liu, L. Jiang, *Adv. Mater.* **2014**, *26*, 4889 – 4894.
[89] K. Murata, K. Mitsuoka, T. Hirai, T. Walz, P. Agre, J. B. Heymann, A. Engel, Y. Fujiyoshi, *Nature* **2000**, *407*, 599 – 605.
[90] A. Anishkin, V. Gendel, N. A. Sharifi, C. S. Chiang, L. Shirinian, H. R. Guy, S. Sukharev, *Biophys. J.* **2004**, *86*, 2883 – 2895.
[91] X. Hou, L. Jiang, *ACS Nano* **2009**, *3*, 3339 – 3342.
[92] L. P. Wen, X. Hou, Y. Tian, F. Q. Nie, Y. L. Song, J. Zhai, L. Jiang, *Adv. Mater.* **2010**, *22*, 1021 – 1024.
[93] X. Hou, W. Guo, L. Jiang, *Chem. Soc. Rev.* **2011**, *40*, 2385 – 2401.
[94] L. Wen, Y. Tian, J. Ma, J. Zhai, L. Jiang, *Phys. Chem. Chem. Phys.* **2012**, *14*, 4027 – 4042.
[95] H. J. Bakker, J. J. Gilijamse, A. J. Lock, *Proc. Natl. Acad. Sci. USA* **2005**, *102*, 3202 – 3207.
[96] O. Beckstein, P. C. Biggin, M. S. P. Sansom, *J. Phys. Chem. B* **2001**, *105*, 12902 – 12905.
[97] G. Hummer, J. C. Rasaiah, J. P. Noworyta, *Nature* **2001**, *414*, 188 – 190.
[98] E. Tajkhorshid, P. Nollert, M. Ø. Jensen, L. J. W. Miercke, J. O′Connell, R. M. Stroud, K. Schulten, *Science* **2002**, *296*, 525 – 530.
[99] Z. S. Siwy, *Adv. Funct. Mater.* **2006**, *16*, 735 – 746.
[100] W. Guo, H. W. Xia, F. Xia, X. Hou, L. X. Cao, L. Wang, J. M. Xue, G. Z. Zhang, Y. L. Song, D. B. Zhu, Y. G. Wang, L. Jiang, *ChemPhysChem* **2010**, *11*, 859 – 864.
[101] I. Vlassiouk, C.-D. Park, S. A. Vail, D. Gust, S. Smirnov, *Nano Lett.* **2006**, *6*, 1013 – 1017.
[102] L. Wen, X. Hou, Y. Tian, J. Zhai, L. Jiang, *Adv. Funct. Mater.* **2010**, *20*, 2636 – 2642.
[103] W. Guo, L. X. Cao, J. C. Xia, F. Q. Nie, W. Ma, J. M. Xue, Y. L. Song, D. B. Zhu, Y. G. Wang, L. Jiang, *Adv. Funct. Mater.* **2010**, *20*, 1339 – 1344.
[104] E. N. Savariar, K. Krishnamoorthy, S. Thayumanavan, *Nat. Nanotechnol.* **2008**, *3*, 112 – 117.
[105] B. Yameen, M. Ali, R. Neumann, W. Ensinger, W. Knoll, O. Azzaroni, *Small* **2009**, *5*, 1287 – 1291.
[106] M. Zhang, X. Hou, J. Wang, Y. Tian, X. Fan, J. Zhai, L. Jiang, *Adv. Mater.* **2012**, *24*, 2424 – 2428.
[107] X. Hou, F. Yang, L. Li, Y. L. Song, L. Jiang, D. B. Zhu, *J. Am. Chem. Soc.* **2010**, *132*, 11736 – 11742.
[108] L. Wen, L. Jiang, *Natl. Sci. Rev.* **2014**, *1*, 144 – 156.
[109] F. H. J. van der Heyden, D. J. Bonthuis, D. Stein, C. Meyer, C. Dekker, *Nano Lett.* **2006**, *6*, 2232 – 2237.
[110] L. Wen, Y. Tian, Y. Guo, J. Ma, W. Liu, L. Jiang, *Adv. Funct. Mater.* **2013**, *23*, 2887 – 2893.
[111] J. Gao, W. Guo, D. Feng, H. Wang, D. Zhao, L. Jiang, *J. Am. Chem. Soc.* **2014**, *136*, 12265 – 12272.
[112] W. Guo, C. Cheng, Y. Wu, Y. Jiang, J. Gao, D. Li, L. Jiang, *Adv. Mater.* **2013**, *25*, 6064 – 6068.
[113] L.-Q. Gu, O. Braha, S. Conlan, S. Cheley, H. Bayley, *Nature* **1999**, *398*, 686 – 690.
[114] S. M. Bezrukov, I. Vodyanoy, R. A. Brutyan, J. J. Kasianowicz, *Macromolecules* **1996**, *29*, 8517 – 8522.
[115] L. Movileanu, S. Howorka, O. Braha, H. Bayley, *Nat. Biotechnol.* **2000**, *18*, 1091 – 1095.
[116] X. Hou, W. Guo, F. Xia, F. Q. Nie, H. Dong, Y. Tian, L. P. Wen, L. Wang, L. X. Cao, Y. Yang, J. M. Xue, Y. L. Song, Y. G. Wang, D. S. Liu, L. Jiang, *J. Am. Chem. Soc.* **2009**, *131*, 7800 – 7805.
[117] Y. Tian, X. Hou, L. Wen, W. Guo, Y. Song, H. Sun, Y. Wang, L. Jiang, D. Zhu, *Chem. Commun.* **2010**, *46*, 1682 – 1684.
[118] Y. Tian, Z. Zhang, L. Wen, J. Ma, Y. Zhang, W. Liu, J. Zhai, L. Jiang, *Chem. Commun.* **2013**, *49*, 10679 – 10681.
[119] L. Gao, P. Li, Y. Zhang, K. Xiao, J. Ma, G. Xie, G. Hou, Z. Zhang, L. Wen, L. Jiang, *Small* **2014**, DOI: 10.1002/smll.201400658.
[120] C. P. Han, X. Hou, H. C. Zhang, W. Guo, H. B. Li, L. Jiang, *J. Am. Chem. Soc.* **2011**, *133*, 7644 – 7647.